

CONFERENCE RECORD OF THE TWENTY FIFTH IEEE PHOTOVOLTAIC SPECIALISTS CONFERENCE - 1996

HYATT REGENCY CRYSTAL CITY
WASHINGTON, DC
MAY 13-17, 1996



SPONSORED BY THE IEEE ELECTRON DEVICES SOCIETY (USA)



Copyright and Reprint Permission: Abstracting is permitted with credit to the source. Libraries are permitted to photocopy beyond the limit of U.S. copyright law for private use of patrons those articles in this volume that carry a code at the bottom of the first page, provided the per-copy fee indicated in the code is paid through Copyright Clearance Center, 27 Congress Street, Salem, MA 01970. For other copying, reprint or republication permission, write to IEEE Copyrights Manager, IEEE Service Center, 445 Hoes Lane, P.O. Box 1331, Piscataway, NJ 08855-1331. All rights reserved.

Copyright © 1996 by the Institute of Electrical and Electronics Engineers, Inc.

TWENTY-FIFTH IEEE PHOTOVOLTAIC SPECIALISTS CONFERENCE - 1996

IEEE Catalog Number:	**96CH35897**	
ISBN:	**0-7803-3166-4**	**Softbound Edition**
	0-7803-3167-2	**Casebound Edition**
	0-7803-3168-0	**Microfiche Edition**
Library of Congress:	**84-640812**	
ISSN:	**0160-8371**	

TABLE OF CONTENTS

CHERRY AWARD ADDRESS

Solar Electric Power for a Better Tomorrow 1
A.M. Barnett

INTERNATIONAL PROGRAMS

Super-High Efficiency Solar Cell R&D Program in Japan 9
M. Yamaguchi and S. Wakamatsu

The Swiss 1 MWp PV-School Demonstration Program 13
Th. Nordmann

PV Applications in Australia 19
M. Watt

1. III-V MATERIALS AND DEVICES

A Review of Recent Advances in Thermophotovoltaics 25
T.J. Coutts, M.W. Wanlass, J.S. Ward and S. Johnson

18.2% (AM1.5) Efficient GaAs Solar Cell on Optical-Grade Polycrystalline Ge Substrate 31
R. Venkatasubramanian, B.C. O'Quinn, J.S. Hills, P.R. Sharps, M.L. Timmons, J.A. Hutchby, H. Field, R. Ahrenkiel and B. Keyes

Hidden But Important Parameters in $Ga_{0.5}In_{0.5}P$ Cell Growth 37
S.R. Kurtz, J.M. Olson, K.A. Bertness, K. Sinha, B. McMahon and S. Asher

Monolithically Interconnected InGaAs TPV Module Development 43
D.M. Wilt, N.S. Fatemi, P.P. Jenkins, R.W. Hoffman, Jr., G.A. Landis and R.K. Jain

High-Power Density (1040 W/kg) GaAs Cells for Ultralight Aircraft 49
S. Wojtczuk and K. Reinhardt

Thin Film GaAs Solar Cells on Glass Substrates by Epitaxial Liftoff 53
X.Y. Lee, A.K. Verma, C.Q. Wu, M. Goertemiller, E. Yablonovitch, J. Eldredge and D. Lillington

Large Area, Thin Film Epitaxial Lift Off III/V Solar Cells 57
P.R. Hageman, G.J. Bauhuis, A. van Geelen, P.C. van Rijsingen, J.J. Schermer and L.J. Giling

GaAs Solar Cells Grown on GaP 61
L.C. Olsen, X. Deng, W. Lei, F.W. Addis and J. Li

ZnSe Window Layers for GaAs Solar Cells 65
J.A. Yater, G.A. Landis, S.G. Bailey, L.C. Olsen and F.W. Addis

A Computational Approach to the Analysis of Distributed Bragg Reflectors in Direct-Gap Solar Cells 69
S.M. Durbin

On-Sun Concentrator Performance of GaInP/GaAs Tandem Cells 73
D.J. Friedman, S.R. Kurtz, K. Sinha, W.E. McMahon, C.M. Kramer, J.M. Olson, J.B. Lasich, A.X. Cleeve and I. Connaughton

Production Data on 0.55 eV InGaAs Thermophotovoltaic Cells 77
S. Wojtczuk, P. Colter, G. Charache and B. Campbell

Recent Progress in InGaAsSb/GaSb TPV Devices 81
Z.A. Shellenbarger, M.G. Mauk, L.C. DiNetta and G.W. Charache

Ultra-Low Resistance, Nondestructive Contact System for InP/InGaAs/InP Double Heterostructure TPV Devices 85
N.S. Fatemi, V.G. Weizer, D.M. Wilt and R.W. Hoffman, Jr.

Modelling of Tandem Cell Temperature Coefficients 89
D.J. Friedman

Silicon Carbide Alphavoltaic Battery 93
G. Rybicki, C. Vargas-Aburto and R. Uribe

Molecular Beam Epitaxy Grown GaInP Top Cells and GaAs Tunnel Diodes for Tandem Applications 97
J. Lammasniemi, K. Tappura, R. Jaakkola, A. Kazantsev, K. Rakennus, P. Uusimaa and M. Pessa

GaAs Converter for High Power Laser Diode 101
A. Fave, A. Kaminski, M. Gavand, L. Mayet and A. Laugier

Analysis of Heteroepitaxial ALGAAS/SI Tandem Solar Cell for Concentrator Applications 105
M.-J. Yang, S.J. Taylor and M. Yamaguchi

Use of High Back Surface Reflectance in PV Cell Design 109
P.A. Iles and C.L. Chu

A New Approach to P-Doping and the Observation of Efficiency Enhancement in InP/InGaAs Quantum Well Solar Cells 113
A. Zachariou, K.W.J. Barnham, P. Griffin, J. Nelson, C. Button, M. Hopkinson, M. Pate and J. Epler

GaAs- and InAlGaAs-Based Concentrator-Type Cells for Conversion of Power Transmitted by Optical Fibers 117
A.L. Fahrenbruch, A. Lopez-Otero, J.G. Werthen and T.-C. Wu

Development of the GaAs Solar Cell for Space Application 121
C. Mingbo and Z. Zhongwei

Hydrocarbon Fired Thermophotovoltaic Generator Prototypes Using Low Bandgap Gallium Antimonide Cells 125
L. Fraas, H.H. Xiang, J. Samaras, R. Ballantyne, D. Williams, S. Hui and L. Ferguson

The Combined Photovoltaic Converters Based on Gallium Arsenide for Space Application 129
M. Kagan, V. Letin and T. Nuller

GaSb-Based (Thermo)Photovoltaic Cells with Zn Diffused Emitters 133
A.W. Bett, S. Keser, G. Stollwerck, O.V. Sulima and W. Wettling

Current Status of Low-Temperature Radiator Thermophotovoltaic Devices 137
G.W. Charache, J.L. Egley, L.R. Danielson, D.M. DePoy, P.F. Baldasaro, B.C. Campbell, S. Hui, L.M. Fraas and S.J. Wojtczuk

Non-Destructive Testing by Absolute Room Temperature Photoluminescence Quantum Efficiency of GaAs Solar Cells 141
X.Y. Lee, C.Q. Wu, A.K. Verma, R. Ranganathan and E. Yablonovitch

GaAs and GaSb Based Solar Cells for Concentrator and Thermophotovoltaic Applications 143
V.M. Andreev, V.P. Khvostikov, E.V. Paleeva, S.V. Sorokina and M.Z. Shvarts

"Buried" Metal/Dielectric/Semiconductor Reflectors for Light Trapping in Epitaxial Thin-Film Solar Cells 147
M.G. Mauk, P.A. Burch, S.W. Johnson, T.A. Goodwin and A.M. Barnett

2. SPACE SOLAR CELLS

Radiation-Hard, Lightweight 12% AM0 BOL InP/Si Solar Cells 151
S. Wojtczuk, P. Colter, N.H. Karam, H.B. Serreze, G.P. Summers and R.J. Walters

Flexible and Light Weight Copper Indium Diselenide Solar Cells 157
B.M. Başol, V.K. Kapur, C.R. Leidholm and A. Halani

Radiation-Resistance of INGAP Solar Cells 163
M. Yamaguchi, C. Vargas-Aburto, S.J. Taylor, M.-J. Yang, T. Takamoto, E. Ikeda, H. Kurita, M. Ohmori, R.M. Uribe, D. Brinker and D.A. Scheiman

Analysis of Damage to Silicon Solar Cells by High Fluence Electron Irradiation 167
M. Yamaguchi, S.J. Taylor, S. Matsuda, O. Kawasaki and K. Ando

Development of High Efficiency p^+/n InP Solar Cells for Hetero-Epitaxial Applications 171
R.W. Hoffman Jr., N.S. Fatemi, P.P. Jenkins, D.A. Scheiman, S.A. Ringel, W. Davis, V.G. Weizer, D.M. Wilt and D.J. Brinker

Development of P/N and N/P Thick Emitter InP Solar Cells 175
P.R. Sharps, M.L. Timmons, S.R. Messenger, H.L. Cotal, G.P. Summers and P.A. Iles

A Comparison of Hydrogen Passivation in Heteroepitaxial N^+P and P^+N Solar Cells 179
B. Chatterjee, S.A. Ringel and R. Hoffman, Jr.

Experimental Results of $GaInP_2$/GaAs/Ge Triple Junction Cell Development for Space Power Systems 183
P.K. Chiang, J.H. Ermer, W.T. Nishikawa, D.D. Krut, D.E. Joslin, J.W. Eldredge, B.T. Cavicchi and J.M. Olson

Production Experience with Large Area, Dual Junction Space Cells 187
Y.C.M. Yeh, C.L. Chu, J. Krogen, F.F. Ho, G.C. Datum, S. Billets, J.M. Olson and M.L. Timmons

Lightweight, Light-Trapped, Thin GaAs Solar Cell for Spacecraft Applications: Progress and Results Update 191
M.H. Hannon, M.W. Dashiell, L.C. DiNetta and A.M. Barnett

Final Results from the PASP Plus Flight Experiment 195
H. Curtis and D. Marvin

Results of Three Recent GaAs Flight Experiments: ASCOT, PASP-Plus and STRV-1b 199
D.C. Marvin and M. Gates

Laboratory Instrumentation and Techniques for Characterizing Multi-Junction Solar Cells for Space Applications 203
J.R. Woodyard

The Effect of an Applied Electric Field on Defect Introduction Rates in N-Type InP 207
M.J. Panunto and G.P. Summers

Deep Space Degradation of Si and GaAs Solar Cells 211
J.C. Bourgoin, R. Kiliulis, C. Gonzales, G. Strobl, C. Flores, K. Bogus and C. Signorini

High Efficiency Line-Focus Photovoltaic Receivers Using Optical Secondaries for Radiation Resistance 215
J. Avery, K. Kimes, P. Custard, L. Fraas, M. Piszczor and M. O'Neill

Spectral Response of Electron-Irradiated Homoepitaxial InP Solar Cells 219
H.L. Cotal, S.R. Messenger, R.J. Walters and G.P. Summers

A New Proton Irradiation Facility to Investigate the Effect of Test Conditions on Solar Cell Degradation 223
C. Goodbody, R. Kimber and S. Sugden

Development of Back Junction Point Contact Photovoltaic Cells and Arrays for Space 227
V. Garboushian, G. Turner, S. Yoon and G.J. Vendura Jr.

A Novel, Non-Destructive, Technique Using EBIC to Determine Diffusion Lengths in GaAs Solar Cells 231
C. Hardingham

The UoSAT-5 Solar Cell Experiment—Over 4 years in Orbit 235
C. Goodbody and R. Kimber

The Effects of Irradiation on Heteroepitaxial InP/InGaAs Solar Cells 239
L.B. Karlina, V.V. Kozlovskii, V.A. Solov'ev and M.Z. Shvarts

Angle of Incidence Corrections for GaAs/Ge Solar Cells with Low Absorptance Coverglass 243
D.R. Burger, R.L. Mueller, G. Goodelle, J. Powe and J. Schwartz

Lightweight $CuInSe_2$ Space Solar Cells Fabricated by Chemical Thinning 247
N.P. Kim, J.A. Nielsen and M.A. Verzwyvelt

Reverse Bias Characteristics of Modules Made of Solar Cells with and without Integrated Bypass Function (IBF) 251
T. Hisamatsu, O. Kawasaki, S. Matsuda, H. Washio, T. Saga, T. Matsutani and A. Suzuki

Ultrathin GaAs Space Solar Cell Devices 255
C. Hardingham, C.R. Huggins, J.W. Simpson and T.A. Cross

Thin, Lightweight, 18% Efficient Space Silicon Solar Cell and Array 259
S. Yoon, G. Turner and V. Garboushian

Analysis of Lips III Satellite a-Si:H Alloy Solar Cell Data 263
J.R. Woodyard and J.G. Severns

3. SPACE SYSTEMS

Manufacturing Experience with $GaInP_2$/GaAs/Ge Solar Panels for Space Demonstration 267
E.B. Linder and J.P. Hanley

The AstroEdge* Solar Array for the NASA Small Spacecraft Technology Initiative "Clark" Satellite 271
J.T. Renshall and G.W. Marks

GaAs Solar Panels for Small Satellites: Performance Data and Technology Trends 277
T.A. Cross, C.M. Hardingham, C.R. Huggins and S.P. Wood

Mars Global Surveyor (MGS) High Temperature Survival Solar Array 283
P.M. Stella, R.G. Ross, Jr., B.S. Smith, G.S. Glenn and K.S. Sharmit

Application of Extreme Value Statistics to the Prediction of Solar Flare Proton Effects on Solar Cells 289
G.P. Summers, M.A. Xapsos and E.A. Burke

Cost Performance of Multi-Junction, Gallium Arsenide and Silicon Solar Cells on Spacecraft 293
E.M. Gaddy

Advanced Solar Panel Designs 297
E.L. Ralph and E.B. Linder

The First Solar Array with 5 μm GaAs Solar Cells 301
H. Bebermeier, H. Bröker and K.-H. Wehner

The GGS Spacecraft, Solar Arrays for Space Physics 305
T. Spitzer

Environmental Testing of Chemically Thinned, Lightweight $CuInSe_2$ Solar Cells 309
N.P. Kim, M.A. Verzwyvelt, M. Thompson and K. Coates

Solar Array Passive Functional Tests 313
R.L. Mueller and D.R. Burger

Low Intensity Low Temperature (LILT) Measurements and Coefficients of New Photovoltaic Structures 317
P.P. Jenkins, D.A. Scheiman, D.J. Brinker and J. Appelbaum

The Development of High Efficiency Flexible Solar Array Paddle of Adeos-II 321
Y. Kojima, T. Tamura, Y. Nozaki and Y. Onishi

Magnetic Field Cancellation Techniques for the Mars Global Surveyor Solar Array 325
M.H. Acuña, J.L. Scheifele, P. Stella, C. Kloss, B. Smith, G. Heinsohn and K. Sharmit

Lessons Learned About Fabrication of Space Solar Arrays from Thermal Cycle Failures 329
I.N. Blake III

The Design, Qualification and Use of Bypass Diode Integration Onto GaAs/Ge Solar Cells 333
R.B. Dally, J.R. Kukulka and J.A. Schwartz

CdTe Terrestrial Modules as a Power Source for a Regenerative Fuel Cell Power Plant for Space Applications 337
H.S. Edwards, G.D. Smith, G. Voecks, N. Rohatgi, P. Prokopius, K. Zweibel and J.F. Hoelscher

Development of PV Receivers for Space Line-Focus Concentrator Modules 341
V.M. Andreev, V.M. Lantratov, V.R. Larionov, V.D. Rumyantsev and M.Z. Shvarts

Indoor and Outdoor Testing of Space Concentrator AlGaAs/GaAs Photovoltaic Modules with Fresnel Lenses 345
V.A. Grilikhes, V.D. Rumyantsev and M.Z. Shvarts

Line-Focus Optics for Multijunction Cells in Space Power Arrays 349
M.J. O'Neill

The Scarlet Light Concentrating Solar Array 353
D.M. Allen, P.A. Jones, D.M. Murphy and M.F. Piszczor

Design and Manufacturing Experience with GaAs/Ge Solar Cells as Gained with the Tempo Solar Generator Program 357
W.D. Schultze

Estimating and Controlling Chromatic Aberration Losses for Two-Junction, Two-Terminal Devices in Refractive Concentrator Systems 361
S.R. Kurtz and M.J. O'Neill

4. SILICON MATERIALS AND DEVICES

Crystalline Silicon Films by Chemical Vapor Deposition on Glass for Thin Film Solar Cells 365
R.B. Bergmann, R. Brendel, M. Wolf, P. Lölgen, J.H. Werner, J. Krinke and H.P. Strunk

Advances in Low-Temperature Passivated Silicon Solar Cells 371
A.G. Aberle and R. Hezel

PC1D Version 4 for Windows: From Analysis to Design 377
P.A. Basore and D.A. Clugston

The Coming of Age of a New PV Wafer Technology—Some Aspects of EFG Polycrystalline Silicon Sheet Manufacture 383
M.J. Kardauskas, M.D. Rosenblum, B.H. Mackintosh and J.P. Kalejs

Simplified Buried Contact Solar Cell Process 389
S.R. Wenham, C.B. Honsberg, S. Edmiston, L. Koschier, A. Fung, M.A. Green and F. Ferrazza

A Novel Technology for the Simultaneous Diffusion of Boron, Aluminum and Phosphorus in Silicon 393
T. Krygowski, P. Sana, G. Crotty and A. Rohatgi

Selective Emitter Formation Using Optical Thermal Heating 397
A. Slaoui, A. Lachiq, L. Ventura and J.C. Muller

Elimination of Parasitic Effects in Floating Junction Rear Surface Passivation for Solar Cells 401
C.B. Honsberg, S.B. Ghozati, A.U. Ebong, Y.-H. Tang and S.R. Wenham

Solar Cells with Efficiencies Above 21% Processed from Czochralski Grown Silicon 405
J. Knobloch, S.W. Glunz, D. Biro, W. Warta, E. Schäffer and W. Wettling

High-Efficiency Cell Structures and Processes Applied to Photovoltaic-Grade Czochralski Silicon 409
J.M. Gee, R.R. King and K.W. Mitchell

Record Low Surface Recombination Velocities on Low-Resistivity Silicon Solar Cell Substrates 413
J. Schmidt, T. Lauinger, A.G. Aberle and R. Hezel

UV Stability of Highest-Quality Plasma Silicon Nitride Passivation of Silicon Solar Cells 417
T. Lauinger, J. Moschner, A.G. Aberle and R. Hezel

High-Efficiency Silicon Solar Cells by Low-Cost Rapid Thermal Processing, Screen Printing and Plasma-Enhanced Chemical Vapor Deposition 421
P. Doshi, J. Mejia, K. Tate, S. Kamra, A. Rohatgi, S. Narayanan and R. Singh

Experimental Investigation of a Field Effect Back Surface Passivation of Silicon Solar Cells 425
Y. Bai, J.E. Phillips and A.M. Barnett

Microcrystalline-Crystalline Silicon Heterojunction Solar Cells Using Highly Conductive Thin P-Type Microcrystalline Silicon Window Layers 429
M.W.M. van Cleef, J.K. Rath, F.A. Rubinelli, C.H.M. van der Werf and R.E.I. Schropp

17.1% Efficient Truncated-Pyramid Inversion-Layer Silicon Solar Cells 433
M. Grauvogl, A.G. Aberle and R. Hezel

Phosphorus and Aluminum Gettering—Investigation of Synergistic Effects in Single-Crystal and Multicrystalline Silicon 437
W.K. Schubert and J.M. Gee

Aluminum Backside Segregation Gettering 441
H. Hieslmair, S. McHugo and E.R. Weber

Combined Characterization of Inhomogeneities in DCM Multicrystalline Silicon Wafers 445
A. Fukatsu, T. Saitoh and I. Hide

The Optimization and Fabrication of High Efficiency HEM Multicrystalline Silicon Solar Cells 449
S. Narasimha, S. Kamra, A. Rohatgi, C.P. Khattak and D. Ruby

Identification of Factors Reducing Voc in MC Silicon Solar Cells 453
O. Breitenstein, K. Iwig and I. Konovalov

Quasi-Steady-State Photoconductance, a New Method for Solar Cell Material and Device Characterization 457
R.A. Sinton, A. Cuevas and M. Stuckings

Porous Silicon Gettering 461
Y.S. Tsuo, P. Menna, J.R. Pitts, K.R. Jantzen, S.E. Asher, M.M. Al-Jassim and T.F. Ciszek

High-Efficiency CVD Multi-Layer Thin-Film Silicon Solar Cells 465
G.F. Zheng, A.B. Sproul, S.R. Wenham and M.A. Green

Numerical Simulation of Innovative Device Structures for Silicon Thin-Film Solar Cells 469
U. Rau, T. Meyer, M. Goldbach, R. Brendel and J.H. Werner

Grain Boundaries in Silicon: Microstructure and Minority Carrier Recombination 473
J. Krinke, M. Albrecht, W. Dorsch, A. Voigt, H.P. Strunk, B. Steiner and G. Wagner

13% Silicon Film® Solar Cells on Low-Cost Barrier-Coated Substrates 477
A.E. Ingram, A.M. Barnett, J.E. Cotter, D.H. Ford, R.B. Hall, J.A. Rand and C.J. Thomas

In-Situ Control in Zone-Melting Recrystallization Process for Formation of High-Quality Thin Film Polycrystalline Si 481
Y. Kawama, A. Takami, H. Naomoto, S. Hamamoto and T. Ishihara

Crystal-Orientation Dependence of Surface Recombination Velocity for Silicon Nitride Passivated Silicon Wafers 485
F.M. Schuurmans, A. Schönecker, J.A. Eikelboom and W.C. Sinke

Cost-Effective Bifacial Silicon Solar Cells with 19% Front and 18% Rear Efficiency 489
A. Hübner, A.G. Aberle and R. Hezel

Fabrication and Characterisation of 662-mV Open-Circuit Voltage High-Efficiency Inversion-Layer Silicon Solar Cells 493
B. Kuhlmann, A.G. Aberle, R. Meyer, A. Hübner, C. Hampe and R. Hezel

Series Resistance in Double-Polysilicon-Contacted Silicon Solar Cells 497
S. Silvestre, D. Parton, L. Castañer, J. Carter and P. Ashburn

Control of Back Surface Reflectance From Aluminum Alloyed Contacts on Silicon Solar Cells 501
M. Cudzinovic and B. Sopori

Dependence of Cell Performance on Wafer Thickness for BSF and Non-BSF Cells 505
T. Koval, J. Wohlgemuth and B. Kinsey

Single Step Rapid Thermal Diffusion for Selective Emitter Formation and Selective Oxidation 509
R. Schindler, A. Breymesser, H. Lautenschlager, C. Marckmann, S. Noël and U. Schubert

Optimization of Boron Groove Diffusion for Double Sided Buried Contact Silicon Solar Cells 513
A.U. Ebong, S.H. Lee, C.B. Honsberg and S.R. Wenham

Improved Geometry of Heavily Diffused Emitters in High-Efficiency Silicon Solar Cells 517
H. Ohtsuka, S. Muramatsu, Y. Nagata, M. Sakamoto, K. Tsutsui, T. Uematsu and T. Warabisako

Mechanically Grooved High-Efficiency Silicon Solar Cells with Self-Aligned Metallisation 521
M. Verbeek, A. Metz, A.G. Aberle and R. Hezel

Highly Efficient Crystalline Silicon Solar Cells Using a Novel Shallow Angle Metallization (SAM) Technique 525
P. Fath, E. Bucher and G. Willeke

Building a Cost-Effective, Fabrication Facility for Silicon Solar Cell R & D and Production 529
R.A. Crane, P.J. Verlinden and R.M. Swanson

Properties of Sputtered Amorphous Silicon/ Crystalline Silicon Solar Cells 533
B. Jagannathan and W.A. Anderson

Quantum Efficiencies Exceeding Unity in Amorphized Silicon Layers 537
Z.T. Kuznicki

Cz Si Photovoltaics: Towards 100 MW 541
K.W. Mitchell, R.R. King and T.L. Jester

Concept for an Online Material Quality Control by Numerical Simulation of a Silicon Ingot Solidification Process 545
D. Franke, I. Steinbach, W. Krumbe, J. Liebermann and W. Koch

Grain Boundary Modeling and Characterization of Thin-Film Silicon Solar Cells 549
A.B. Sproul, S.A. Edmiston, T. Puzzer, G. Heiser, S.R. Wenham, M.A. Green and T.L. Young

Surface Recombination Velocity in Silicon Substrates Determined from Light Beam Induced Current Measurements 553
A. Morales-Acevedo and G. Santana

A Simple Procedure to Analyze Rear-Surface Internal Quantum Efficiency 557
J.M. Gee

Interpretation of the Spectral Response of a Solar Cell in Terms of the Spatial Collection Efficiency 561
J. Sinkkonen, A. Hovinen, T. Siirtola, E. Tuominen and M. Acerbis

Statistical Analysis for Solar Cell Research 565
A.W. Weeber and W.C. Sinke

Improved Treatment of the Strongly Varying Slope in Fitting Solar Cell I-V Curves 569
A.R. Burgers, J.A. Eikelboom, A. Schönecker and W.C. Sinke

Conduction Processes in Silicon Solar Cells 573
A. Kaminski, J.J. Marchand, H. El Omari, A. Laugier, Q.N. Le and D. Sarti

Influence of Baking Conditions of Doped Spin-On Glass Sources on the Formation of Laser Assisted Selective Emitters 577
L. Ventura, J.P. Schunck, J.C. Muller, S. Barthe, U.B. Vetrella, L. Pirozzi and E. Salza

Improved Understanding and Characterisation of Rapid Thermal Oxides 581
J. Horzel, W. Storm, T. Trenkler, S. Sivoththaman, J. Nijs, R. Mertens and G. Adriaenssens

Screen Printed Contacts Formation by Rapid Thermal Annealing in Multicrystalline Silicon Solar Cells 585
H. El Omari, J.P. Boyeaux and A. Laugier

Effect of Porous Silicon Layer Re-Emission on Silicon Solar Cell Photocurrent 589
V.A. Skryshevsky, A. Laugier, V.I. Strikha, V.A. Vikulov and A. Kaminski

Sunalyzer—A Powerful and Cost-Effective Solar Cell I-V Tester for the Photovoltaic Community 593
A.G. Aberle, T. Lauinger, S. Bowden, S. Wegener and G. Betz

Automation in HEM Silicon Ingot Production 597
C.P. Khattak and F. Schmid

High Power, Commercial Silicon-Film® Solar Cells 601
D.H. Ford, A.M. Barnett, R.B. Hall, C.L. Kendall and J.A. Rand

Process Development Toward a 15% Efficient 230 cm^2 Screen Printed Multicrystalline Silicon Solar Cell 605
S. Narayanan, J. Creager, M. Roy and J. Wohlgemuth

Transient Thermal Effects into a 155 KG Polix Ingot 609
A. Laugier, E. Borne, H. El Omari, G. Goaer and D. Sarti

Solidification of Multicrystalline Silicon Ingots: Comparison Between Conventional Casting and Electromagnetic Casting Processes 613
E. Ehret, A. Laugier and H. El Omari

From mc-Si Material Made by Cold Crucible Continuous Pulling to Solar Cells 617
S. Martinuzzi, I. Périchaud, L. Clerc, M. Bacon, F. Floret, D. Sarti, G. Dour, Q.N. Le, G. Goaer and F. Durand

Rapid Thermal Processing of Conventionally and Electromagnetically Cast 100 cm^2 Multicrystalline Silicon 621
S. Sivoththaman, W. Laureys, P. De Schepper, J. Nijs and R. Mertens

A Comparison of Gettering in Single- and Multicrystalline Silicon for Solar Cells 625
B.L. Sopori, L. Jastrzebski and T. Tan

Gettering Effect of Aluminium in mc-Si and c-Si Wafers and in Solar Cells 629
O. Porre, S. Martinuzzi, M. Pasquinelli, I. Périchaud and N. Gay

Localization and Identification of Microscopic Defects Leading to Locally Enhanced Currents Across PN-Junctions of Solar Cells 633
A. Voigt, T. Göbel, H.P. Strunk, C. Hässler, W. Koch, D. Karg and G. Pensl

Optimization of Plasma Deposition and Etching Processes for Commercial Multicrystalline Silicon Solar Cells 637
D.S. Ruby, W.L. Wilbanks, C.B. Fleddermann, M.D. Rosenblum, S. Roncin and S. Narayanan

Open Circuit Voltage Losses in Multicrystalline Silicon: An Investigation by Mini Solar Cells (MSC) 641
R. Baldner, H. Lautenschlager, C. Schetter, R. Schindler and W. Warta

MC-SI Thin Film Solar Cells by Fast CVD On Low Cost SSP Pre-Ribbons 645
F. Faller, N. Schillinger, A. Hurrle, C. Schetter, A. Eyer

Recrystallized Silicon on SIO_2-Layers for Thin Film Solar Cells 649
C. Hebling, R. Gaffke, P. Lanyi, H. Lautenschlager, C. Schetter, B. Wagner and F. Lutz

Interaction Between Bulk and Surface Passivation Mechanisms in Thin Film Solar Cells on Defected Silicon Substrates 653
T. Vermeulen, J. Poortmans, K. Said, O. Evrard, W. Laureys, M. Caymax, J. Nijs, R. Mertens and C. Vinckier

Ceramic Substrates for Thin-Film Crystalline Silicon Solar Cells 657
J.A.M. van Roosmalen, C.J.J. Tool, R.C. Huiberts, R.J.G. Beenen, J.P.P. Huijsmans and W.C. Sinke

Low Temperature Fabrication of Thin Film Polycrystalline Si Solar Cell on the Glass Substrate and its Application to the a-Si:H/Polycrystalline Si Tandem Solar Cell 661
K. Yamamoto, T. Suzuki, M. Yoshimi and A. Nakajima

Initial Results for the Silicon Monolithically Interconnected Solar Cell Product 665
K.P. Shreve, L.C. DiNetta, J.E. Cotter, J.R. Bower, T.R. Ruffins and A.M. Barnett

Scope of VHF Plasma Deposition for Thin-Film Silicon Solar Cells 669
H. Keppner, U. Kroll, P. Torres, J. Meier, D. Fischer, M. Goetz, R. Tscharner and A. Shah

Application of Low-Temperature Electron Cyclotron Resonance CVD to Silicon Thin-Film Solar Cell Preparation 673
P. Müller, I. Beckers, E. Conrad, L. Elstner and W. Fuhs

Surface Recombination at the Si/SiO_2 Overgrowth Interface 677
D.D. Smith, D.J. Aiken and A.M. Barnett

High-Quality Polycrystalline Silicon Layers Grown on Dissimilar Substrates from Metallic Solution 681
I. Silier, M. Konuma, A. Gutjahr and E. Bauser

A Device Structure for Thin, Light Trapped Epitaxial Silicon Solar Cells 685
D.J. Aiken, D.D. Smith and A.M. Barnett

Surface Segregation as a Means of Gettering Cu IN Liquid-Phase-Epitaxy Silicon Thin Layers Grown from AI-Cu-Si Solutions 689
T.H. Wang, T.F. Ciszek, R. Reedy, S. Asher and D. King

High-Efficiency Drift-Field Thin-Film Silicon Solar Cells by Liquid-Phase Epitaxy and Substrate Thinning 693
G.F. Zheng, W. Zhang, Z. Shi, D. Thorp and M.A. Green

Solution Grown Polysilicon for Photovoltaic Devices 697
R.L. Wallace, W.A. Anderson, K.M. Jones and R. Ahrenkiel

Polycrystalline Silicon Thin Films by Rapid Thermal Chemical Vapor Deposition (RTCVD) on Graphite Substrates 701
R. Monna, D. Angermeier, A. Slaoui and J.C. Muller

Absorption Enhancement in Conformally Textured Thin-Film Silicon Solar Cells 705
D. Thorp, P. Campbell and S.R. Wenham

Structural and Optical Properties of Polycrystalline Silicon Thin Films Deposited by PECVD Method 709
F. Zhu, H. Kohara, T. Fuyuki and H. Matsunami

Single-Crystal Si Infrared Improvements 713
Z.T. Kuznicki, L. Wu and E. Christoffel

A Technique for Separating Bulk and Surface Lifetimes in the Analysis of Photoconductance Decay Measurements 717
F.P. Giles and R.J. Schwartz

Development of Easy-to-Use Surface Passivation Schemes for Lifetime Measurements on Monocrystalline Si with (100)-Orientation 721
J. Poortmans, T. Vermeulen, J. Nijs and R. Mertens

A General Two Dimensional Study of the Power Reflection in Microwave Detected Photoconductance Decay Technique for Lifetime Measurement 725
M.Y. Ghannam, S.F. Mahmoud and J.F. Nijs

Determination of Facet Orientations on Alkaline Etched Multicrystalline Wafers 729
J.D. Hylton, A.R. Burgers, R. Kinderman and W.C. Sinke

Optimization of Textured-Dielectric Coatings for Crystalline-Silicon Solar Cells 733
J.M. Gee, R. Gordon and H. Liang

Properties of Iron-Doped Multicrystalline Silicon Grown by the Float-Zone Technique 737
T.F. Ciszek, T.H. Wang, R.K. Ahrenkiel and R. Matson

Record High 18.6% Efficient Solar Cell on HEM Multicrystalline Material 741
A. Rohatgi, S. Narasimha, S. Kamra, P. Doshi, C.P. Khattak, K. Emery and H. Field

5. II-VI MATERIALS AND DEVICES

Progress and Issues in Polycrystalline Thin-Film PV Technologies 745
K. Zweibel, H.S. Ullal and B. von Roedern

CDS Films Prepared by the Close-Spaced Sublimation and Their Influence on CDTE/CDS Solar Cell Performance 751
C.S. Ferekides, D. Marinskiy, S. Marinskaya, B. Tetali, D. Oman and D.L. Morel

Thin Film Solar Modules Based on CIS Prepared by the Co-Evaporation Method 757
B. Dimmler, E. Gross, R. Menner, M. Powalla, D. Hariskos, M. Ruckh, U. Rühle and H.W. Schock

Characterization of $Cu(InGa)Se_2$ Solar Cells with High GA Content 763
W.N. Shafarman, R. Klenk and B.E. McCandless

Optimization of Laser Scribing for Thin-Film Photovoltaics 769
A.D. Compaan, I. Matulionis, M.J. Miller and U.N. Jayamaha

Thin Film Cadmium Telluride-Cadmium Sulfide Alloys and Devices 773
D.G. Jensen, B.E. McCandless and R.W. Birkmire

The Role of Oxygen in CdS/CdTe Solar Cells Deposited by Close-Spaced Sublimation 777
D.H. Rose, D.H. Levi, R.J. Matson, D.S. Albin, R.G. Dhere and P. Sheldon

Vapor Phase Treatment of CdTe/CdS Thin Films With $CdCl_2$:O_2 781
B.E. McCandless, H. Hichri, G. Hanket and R.W. Birkmire

Stability Testing of CdTe/CdS Thin-Film Photovoltaic Modules 785
R.C. Powell, R. Sasala, G. Rich, M. Steele, K. Bihn, N. Reiter, S. Cox and G. Dorer

Stress Testing of CdTe Solar Cells 789
P.V. Meyers and J.E. Phillips

$Cu(InGa)Se_2$ Thin-Film Solar Cells With Continuously Evaporated Cd-Free Buffer Layers 793
Y. Ohtake, M. Ichikawa, T. Okamoto, A. Yamada, M. Konagai and K. Saito

Investigations Into Alternative Substrate, Absorber and Buffer Layer Processing for $Cu(In,Ga)Se_2$-Based Solar Cells 797
J.R. Tuttle, T.A. Berens, J. Keane, K.R. Ramanathan, J. Granata, R.N. Bhattacharya, H. Wiesner, M.A. Contreras and R. Noufi

Small- and Large-Area CIGS Modules by Co-Evaporation 801
E. Niemi, J. Hedström, T. Martinsson, K. Granath, L. Stolt, J. Skarp, D. Hariskos, M. Ruckh and H.W. Schock

Diffusion of In and Ga In Selenized Cu-In and Cu-Ga Precursors 805
M. Marudachalam, H. Hichri, R.W. Birkmire, J.M. Schultz, A.B. Swartzlander and M.M. Al-Jassim

Defect Chalcopyrite $Cu(In_{1-X}Ga_X)_3Se_5$ Materials and High-Ga-Content $Cu(In,Ga)Se_2$-Based Solar Cells 809
M.A. Contreras, H. Wiesner, D. Niles, K. Ramanathan, R. Matson, J. Tuttle, J. Keane and R. Noufi

$Cu(In,Ga)Se_2$ Based Submodule Process Robustness 813
J. Kessler, S. Wiedeman, L. Russell, J. Fogleboch, S. Skibo, R. Arya and D. Carlson

Photoluminescence and Photoluminescence Excitation Studies on $CuInSe_2$ Absorber Layers for Solar Cells 817
S. Zott, K. Leo, M. Ruckh and H.-W. Schock

Effects of Buffer Layer Processing on CIGS Excess Carrier Lifetime: Application of Dual-Beam Optical Modulation to Process Analysis 821
S.S. Li, B.J. Stanbery, C.H. Huang, C.H. Chang, Y.S. Chang and T.J. Anderson

Applications of ZnO in $Cu(In,Ga)Se_2$ Solar Cells 825
M. Ruckh, D. Hariskos, U. Rühle, H.W. Schock, R. Menner and B. Dimmler

Thin-Film Module Measurement Artifacts 829
I.L. Eisgruber

Determination of the Valence-Band Offset of CdS/CIS Solar Cell Devices by Target Factor Analysis 833
D.W. Niles, M. Contreras, K. Ramanathan and R. Noufi

Effect of Heat Treatments and Window Layer Processing on the Characteristics of $CuInGaSe_2$ Thin Film Solar Cells 837
K. Ramanathan, M.A. Contreras, J.R. Tuttle, J. Keane, J. Webb, S. Asher, D. Niles, R. Dhere, A.L. Tennant, F.S. Hasoon and R. Noufi

Determination of the Internal Series Resistance of CIS and CIGS Photovoltaic Cell Structures 841
A.E. Delahoy and A.M. Payne

Nucleation and Growth of the CdS Buffer Layer on $Cu(In,Ga)Se_2$ Thin Films 845
T.M. Friedlmeier, D. Braunger, D. Hariskos, M. Kaiser, H.N. Wanka and H.W. Schock

Thermodynamic Assessment of the Cu-In-Se System and Application to Thin Film Photovoltaics 849
C.H. Chang, A. Davydov, B.J. Stanbery and T.J. Anderson

Effect of CdS Thickness on CdS/CdTe Quantum Efficiency 853
J.E. Granata, J.R. Sites, G. Contreras-Puente and A.D. Compaan

Determination of Minority Carrier Lifetimes in $CuInSe_2$ Solar Cell Absorbers 857
K. Puech, S. Zott, K. Leo, M. Ruckh and H.-W. Schock

Influence of Humidity on Polycrystalline $Cu(In,Ga)Se_2$ Thin Films for Solar Cells: A Study of Na and H_2O Coadsorption 861
C. Heske, G. Richter, Z. Chen, R. Fink, E. Umbach, W. Riedl and F. Karg

Physical and Chemical Pathways for Economic Recycling of Cadmium Telluride Thin-Film Photovoltaic Modules 865
R.A. Sasala, J. Bohland and K. Smigielski

Performance vs. Microstructure in RF Sputtered CdS/CdTe Solar Cells 869
M. Shao, U. Jayamaha, E. Bykov, C.N. Tabory and A.D. Compaan

Fabrication of High Efficiency CdTe Thin Film Solar Cells Using Electrodeposition 873
W. Song, D. Mao, Y. Zhu, J. Tang and J.U. Trefny

Monograin Layers and Membranes for Photovoltaics 877
M. Altosaar, T. Varema, M. Deppe, C. Wirts, J. Deppe, J. Hiie, R. Hiesgen, E. Mellikov and D. Meissner

ZnO/ZnO:Al Window and Contact Layer for Thin Film Solar Cells: High Rate Deposition by Simultaneous RF and DC Magnetron Sputtering 881
K. Ellmer, R. Wendt and R. Cebulla

Front Contact Optimization for $Cu(In,Ga)Se_2$ (Sub)Modules 885
J. Kessler, S. Wiedeman, L. Russell, J. Fogleboch, S. Skibo, R. Arya and D. Carlson

Manufacturing-Compatible Methods for the Formation of $Cu(In,Ga)Se_2$ Thin Films 889
A.M. Gabor, J.S. Britt, A.E. Delahoy, R. Noufi and Z.J. Kiss

Superstrate-Type $CuInSe_2$ Thin Film Solar Cells with Selenide Buffer Layers 893
T. Nakada, T. Kume and A. Kunioka

Gallium Content Enhancement in $CuIn_{1-x}Ga_xSe_2$ Thin Films Prepared by Two-Selenizations Process Using Se Vapor 897
N.G. Dhere and K.W. Lynn

Numerical Modelling of ac-Characteristics of CdTe and CIS Solar Cells 901
A. Niemegeers and M. Burgelman

Interpretation of Capacitance-Voltage Characteristics in Thin-Film Solar Cells Using a Detailed Numerical Model 905
J.L. Gray

Dielectric Spectroscopy of Relaxation Processes in $Cu(In,Ga)Se_2$ Solar Cells 909
M. Schmitt, U. Rau, J. Parisi, W. Riedl, J. Rimmasch and F. Karg

Dynamics of Photoexcited Carrier Relaxation and Recombination in CdTe/CdS Thin Films 913
D.H. Levi, B.D. Fluegel, R.K. Ahrenkiel, A.D. Compaan and L.M. Woods

Direct Current-Voltage Measurements of the $Mo/CuInSe_2$ Contact on Operating Solar Cells 917
W.N. Shafarman and J.E. Phillips

Interdiffusion of CdS/CdTe in Laser-Deposited and RF Sputtered Alloys, Bilayers and Solar Cells 921
A. Fischer, C. Narayanswamy, D.S. Grecu, E. Bykov, S.A. Nance, U.N. Jayamaha, G. Contreras-Puente, A.D. Compaan, M.A. Stan and A.R. Mason

The Properties and Optimization of ZnTe:Cu Back Contacts on CdTe/CdS Thin Film Solar Cells 925
J. Tang, D. Mao, L. Feng, W. Song and J.U. Trefny

High-Quality CdTe Films from Nanoparticle Precursors 929
D.L. Schulz, M. Pehnt, E. Urgiles, D.W. Niles, K.M. Jones, C.J. Curtis and D.S. Ginley

Enhanced Performance of CdS/CdTe Thin-Film Devices Through Temperature Profiling Techniques Applied to Close-Spaced Sublimation Deposition 933
X. Li, P. Sheldon, H. Moutinho and R. Matson

Low Resistance Contact to CdTe Thin Films 937
M. Florez, W. de la Cruz, P. Teheran, L. Cota and G. Gordillo

Electrodeposition of Mercury Zinc Telluride Thin Films for Solar Cell Applications 941
C. Thero and P. Singh

Growth Analysis of Cadmium Sulfide Thin Films by Atomic Force Microscopy 945
H.R. Moutinho, R.G. Dhere, K. Ramanathan, P. Sheldon and L.L. Kazmerski

Quantitative Investigation of Reactions in Copper-Indium-Gallium Multilayer Thin Films 949
K.A. Lindahl, D.L. Olson, J.J. Moore, A.B. Swartzlander and R. Noufi

Thin-Film CdS/CdTe Solar Cell with 15.05% Efficiency 953
T. Nishio, K. Omura, A. Hanafusa, T. Arita, H. Higuchi, T. Aramoto, S. Shibutani, S. Kumazawa, M. Murozono, Y. Yabuuchi and H. Takakura

Junction Mechanisms in CDS/CDTE Solar Cells 957
D.M. Oman, S. Karthikeyan, C.S. Ferekides and D.L. Morel

An Experimental and Computer Simulation Study of the Role of CDS in CIS-Type Solar Cells 961
J. Hou, S.J. Fonash and J. Kessler

Siemens Solar CIS Photovoltaic Module and System Performance at the National Renewable Energy Laboratory 965
T. Strand, B. Kroposki, R. Hansen and D. Willett

Technical Evaluation of Solar Cells, Inc. CdTe Module and Array at NREL 969
B. Kroposki, T. Strand, R. Hansen, R. Powell and R. Sasala

Junction Electroluminiscence of $Cu(In,Ga)Se_2$ Devices 973
J.L. Hernández and A. Rockett

Doe/Oer-Sponsored Basic Research in High-Efficiency Photovoltaics 977
S.K. Deb and J.P. Benner

Reaction Analysis of the Formation of CIS at Temperatures from 250 to 400°C 981
N. Orbey, H. Hichri, R.W. Birkmire and T.W.F. Russell

Na Incorporation and Diffusion in $CuIn_{1-x}Ga_xSe_2$ 985
A. Rockett, M. Bodegård, K. Granath and L. Stolt

The Role of $Cu(InGa)(SeS)_2$ Surface Layer on a Graded Band-Gap $Cu(InGa)Se_2$ Thin-Film Solar Cell Prepared by Two-Stage Method 989
K. Kushiya, S. Kuriyagawa, T. Kase, M. Tachiyuki, I. Sugiyama, Y. Satoh, M. Satoh and H. Takeshita

Optical Properties and Defect Levels in a Surface Layer Found on $CuInSe_2$ Thin Films 993
F. Abulfotuh, T. Wangensteen, R. Ahrenkiel and L.L. Kazmerski

CIS Solar Cells with ZnO Buffer Layers 997
L.C. Olsen, H. Aguilar, F.W. Addis, W. Lei and J. Li

Improved Open Circuit Voltage in $CuInS_2$-Based Solar Cells 1001
D. Braunger, Th. Dürr, D. Hariskos, Ch. Köble, Th. Walter, N. Wieser and H.W. Schock

Influence of Na and S Incorporation on the Electronic Transport Properties of $Cu(In,Ga)Se_2$ Solar Cells 1005
U. Rau, M. Schmitt, D. Hilburger, F. Engelhardt, O. Seifert, J. Parisi, W. Riedl, J. Rimmasch and F. Karg

Properties of $CuInS_2$ Thin Films for Solar Cells Prepared by Spray Pyrolysis 1009
M. Ortega-López and A. Morales-Acevedo

HCI Vapor Post-Deposition Heat Treatment of CdTe/CdS Films 1013
Y. Qu, P.V. Meyers and B.E. McCandless

6. AMORPHOUS SILICON MATERIALS AND DEVICES

Amorphous Silicon Alloy Solar Cells and Modules—Opportunities and Challenges 1017
S. Guha

Commercialization of Multijunction Amorphous Silicon Modules 1023
D.E. Carlson, R.R. Arya, M. Bennett, L.-F. Chen, K. Jansen, Y.-M. Li, J. Newton, K. Rajan, R. Romero, D. Talenti, E. Twesme, F. Willing and L. Yang

Control of Plasma and Surface Conditions for Low Defect Density A-SI:H at High Growth Rates 1029
A. Matsuda

Characterization of Amorphous Silicon Solar Cell Preparation Processes by Real Time Spectroscopic Ellipsometry 1035
R.W. Collins, J. Koh, Y. Lu, S. Kim, J.S. Burnham and C.R. Wronski

Progress in Triple-Junction Amorphous Silicon Alloy Solar Cells with Improved Current Mismatch in Component Cells 1041
J. Yang, X. Xu, A. Banerjee and S. Guha

Film-Substrate a-Si Solar Cells and Their Novel Process Technologies 1045
S. Fujikake, K. Tabuchi, A. Takano, T. Wada, S. Saito, H. Sato, T. Yoshida, Y. Ichikawa and H. Sakai

Efficiency Evaluation of a-Si and c-Si Solar Cells for Outdoor Use 1049
M. Kameda, S. Sakai, M. Isomura, K. Sayama, Y. Hishikawa, S. Matsumi, H. Haku, K. Wakisaka, M. Tanaka, S. Kiyama, S. Tsuda and S. Nakano

The "Micromorph" Solar Cell: Extending a-Si:H Technology Towards Thin Film Crystalline Silicon 1053
D. Fischer, S. Dubail, J.A. Anna Selvan, N.P. Vaucher, R. Platz, Ch. Hof, U. Kroll, J. Meier, P. Torres, H. Keppner, N. Wyrsch, M. Goetz, A. Shah and K.-D. Ufert

Long Term Behaviour of Passively Heated or Cooled A-SI:H Modules 1057
C. Hof, M. Lüdi, M. Goetz, D. Fischer and A. Shah

Analysis of Optical Enhancement in a-Si n-i-p Solar Cells Using a Detachable Back Reflector 1061
S.S. Hegedus and X. Deng

Hot Wire Deposited Hydrogenated Amorphous Silicon Solar Cells 1065
A.H. Mahan, E. Iwaniczko, B.P. Nelson, R.C. Reedy Jr., R.S. Crandall, S. Guha and J. Yang

Improved Stability in ECR-Deposited A-SI Solar Cells 1069
V. Dalal, S. Kaushal, R. Girvan, S. Hariasra and L. Sipahi

Importance of Charge Defects in a-Si:H Materials and Solar Cell Structures 1073
L. Jiao, H. Liu, S. Semoushikina, Y. Lee and C.R. Wronski

Preparation of High and Low Bandgap Amorphous Silicon by PECVD and Their Application in Solar Cell 1077
S. Ray and S. Hazra

Optimum Front Contact and Growth Conditions for Microcrystalline Silicon Solar Cells from Hot-Wire CVD 1081
M.B. Schubert, H.N. Wanka and H. Brummack

Self-Limiting Growth of Transparent Conductive ZnO Films by Atomic Layer Deposition 1085
B. Sang and M. Konagai

Enhancement of A-SI:H Solar Cell Characteristics by Hydrogen Treatment at P/I Interface Using Photo-CVD Method 1089
J.-H. Jang and K.-S. Lim

The Role of H_2 Dilution in the Deposition of a-Si:H Films and its Effects on the Solar Cell Degradation 1093
P. Siamchai and M. Konagai

Study of Buffer Layer Design in Single Junction Solar Cells 1097
H. Zhu and S.J. Fonash

Development of Amorphous Silicon Based P-I-N Solar Cell in a Superstrate Structure with P-Microcrystalline Silicon as Window Layer 1101
J.K. Rath, C.H.M. van der Werf, F.A. Rubinelli and R.E.I. Schropp

Temperature Dependence of p-i-n HIT Solar Cell Characteristics 1105
J. Furlan, P. Popović, F. Smole and M. Topič

Effects of μc-Si P-Layer on P-I-N a-Si:H Solar Cell Performance 1109
M. Topič, F. Smole and J. Furlan

Field Collapse Due to Band-Tail Charge in Amorphous Silicon Solar Cells 1113
Q. Wang, R.S. Crandall and E.A. Schiff

Density of States Measurements in a P-I-N Solar Cell 1117
R.S. Crandall and Q. Wang

Development of p-Type Microcrystalline Silicon-Carbon Alloy Thin Film at Low Power and its Application in Tunnel Junctions 1121
S. Ray, A. Dasgupta and A.K. Barua

Light-Induced Degradation in Different p-i-n and n-i Schottky Barrier Solar Cell Structures 1125
H. Liu, Y. Lee, T. Jamali-beh, Z. Lu, R. Collins and C.R. Wronski

Effect of Textured Tin Oxide and Zinc Oxide Substrates on the Current Generation in Amorphous Silicon Solar Cells 1129
S. Hegedus, W. Buchanan, X. Liu and R. Gordon

Role of Bandgap Grading for the Performance of a-SiGe:H Based Solar Cells 1133
J. Fölsch, H. Stiebig, F. Finger, B. Rech, D. Ludszien, A. Lambertz and H. Wagner

Stability of Large-Area Amorphous Silicon Alloy Tandem Solar Modules 1137
L. Chen, F. Willing, L. Yang, Y.M. Li, N. Maley, K. Rajan, M. Bennett and R. Arya

Highly Textured ZnO Thin Films and SnO_2/ZnO Bilayer Films Prepared by the Pyrosol Process 1141
J. Song, C. Lee, K. Lim, K. Yoon and K. Yu

Response Time Distribution—A Way to Describe the Photocurrent Transient 1145
P. Popović, S. Grebner, E. Bassanese, F. Smole, J. Furlan and R. Schwarz

Smooth TCO/Glass Substrates and Diffuse Rear Reflectors for Efficient Low Cost Amorphous Silicon-Based Solar Cells 1149
K. Winz, C.M. Fortmann, Th. Eickhoff, C. Beneking, B. Rech, O. Kluth and H. Wagner

Film Uniformity and Substrate-to-Electrode Attachment in Large-Area VHF Glow-Discharge Deposition of a-Si:H 1153
H. Meiling, W.G.J.H.M. van Sark, J. Bezemer, R.E.I. Schropp and W.F. van der Weg

Factors Limiting Further Improvement of A-SIGE:H 1157
T. Ikeda, G. Ganguly and A. Matsuda

Surface Metastable Layer in Amorphous Silicon and its Influence on Material Photoconductivity and Electronic Stability 1161
R.V. Alyoshkin and S.M. Karabanov

Stability of A-SI:H Solar Cells and Corresponding Intrinsic Materials Fabricated Using Hydrogen Diluted Silane 1165
Y. Lee, L. Jiao, H. Liu, Z. Lu, R. Collins and C.R. Wronski

200 μm Thick Encapsulated Amorphous Silicon Solar Cells 1169
B. Crone, A. Payne and S. Wagner

A PV Module with An Active Area Utilization of 99.8% 1173
T. Glatfelter, M. Lycette, E. Akkashian and K. Hoffman

As Grown and Light Soaked Defect Densities in a-Si:H with Sharp Band Tails 1177
G. Ganguly and A. Matsuda

7. TERRESTRIAL MODULES

Progress in Solarex Crystalline Silicon PVMaT Program 1181
J.H. Wohlgemuth, T. Koval, J. Creager, T. Tomlinson, J. Ellis, F. Artigliere, S. Narayanan, J. Posbic, S. Shea, M. Roy, J. Cliber, M. Conway, D. Vanecek, B. Chen and R. Fernandez

The Road to Commercialization in the PV Industry: A Case Study of EFG Technology 1187
E.J. Henderson and J.P. Kalejs

Results of Five Years of Module Qualification Testing to CEC Specification 503 1191
J. Bishop and H. Ossenbrink

World Overview of Building-Integrated Photovoltaics 1197
S.J. Strong

22.3% Efficient Silicon Solar Cell Module 1203
J. Zhao, A. Wang, E. Abbaspour-Sani, F. Yun, M.A. Green and D.L. King

The Euclides Prototype: An Efficient Parabolic Trough for PV Concentration 1207
G. Sala, J.C. Arboiro, A. Luque, J.C. Zamorano, J.C. Miñano, C. Dramsch, T. Bruton and D. Cunningham

Solartrak® Controller Developments for Today's Applications 1211
A.B. Maish, M. O'Neill, R. West and D.S. Shugar

Benefits from the U.S. Photovoltaic Manufacturing Technology Project 1215
R.L. Mitchell, C.E. Witt, H.P. Thomas, L.O. Herwig, D.S. Ruby and C.C. Aldrich

Estimating Service Lifetimes of a Polymer Encapsulant for Photovoltaic Modules from Accelerated Testing 1219
A.W. Czanderna and F.J. Pern

United States Coast Guard Hybrid System Experience on Kodiak Island, Alaska 1223
S. Durand and D. Slagle

Outdoor Performance of Triple Stacked a-Si Photovoltaic Module in Various Geographical Locations and Climates 1227
K. Fukae, C.C. Lim, M. Tamechika, N. Takehara, K. Saito, I. Kajita and E. Kondo

The AC Photovoltaic Module 1231
R.H. Wills, F.E. Hall, S.J. Strong and J.H. Wohlgemuth

Operation of a 10 kW PV Façade with 100 W AC Photovoltaic Modules 1235
W. Knaupp, D. Schekulin, I. Voigtländer, A. Bleil and C. Binder

A PV Module that Emulates an Asphalt Shingle 1239
T. Glatfelter, S. Guha, K. Hoffman, C. Vogeli, J. Yang, K. Younan and J. Wiehagen

PV Glass Curtain Walls Using Color Solar Cells: The Examination of Structures and Integration on Buildings 1243
N. Ishikawa, M. Kanai, I. Hide, T. Nagai, T. Ito, T. Yoshida, T. Nii, K. Tazawa and T. Harada

Performance Analysis of the Northumberland Building Photovoltaic Facade 1247
N.M. Pearsall and A.R. Wilshaw

Thermal Processing of EVA Encapsulants and Effects of Formulation Additives 1251
F.J. Pern and S.H. Glick

Spectroscopic, Scanning Laser Obic and I-V/QE Characterizations of Browned EVA Solar Cells 1255
F.J. Pern, I.L. Eisgruber and R.H. Micheels

UV Stability and Module Testing of Non-Browning Experimental PV Encapsulants 1259
W.H. Holley, Jr., S.C. Agro, J.P. Galica and R.S. Yorgensen

Results of the PEP'93 Intercomparison of Reference Cell Calibrations and Newer Technology Performance Measurements 1263
C.R. Osterwald, S. Anevsky, A.K. Barua, J. Dubard, K. Emery, D. King, J. Metzdorf, F. Nagamine, R. Shimokawa, N. Udayakumar, Y.X. Wang, T. Wittchen, W. Zaaiman, A. Zastrow and J. Zhang

An Assessment of the Results of Calibrating 600 Silicon PV Reference Devices 1267
C. Helmke, W. Zaaiman and H. Ossenbrink

Non Hot-Spot PV Module Using Solar Cells with Bypass Diode Function 1271
H. Yoshioka, S. Nishikawa, S. Nakajima, M. Asai, S. Takeoka, T. Matsutani and A. Suzuki

Temperature Dependence of Photovoltaic Cells, Modules and Systems 1275
K. Emery, J. Burdick, Y. Caiyem, D. Dunlavy, H. Field, B. Kroposki, T. Moriarty, L. Ottoson, S. Rummel, T. Strand and M.W. Wanlass

Long-Term Performance and Reliability of Crystalline Silicon Photovoltaic Modules 1279
G.H. Atmaram, G.G. Ventre, C.W. Maytrott, J.P. Dunlop and R. Swamy

Improved Three-Quadrants Voltage-To-Current Curve Tracer By A LC Load 1283
E. Barbisio

Influence of Shading on Electrical Parameters of Solar Cells 1287
V. Quaschning and R. Hanitsch

Cell Shunt Resistance and Photovoltaic Module Performance 1291
T.J. McMahon, T.S. Basso and S.R. Rummel

PVSIM©: A Simulation Program for Photovoltaic Cells, Modules and Arrays 1295
D.L. King, J.K. Dudley and W.E. Boyson

Refractive Spectrum Splitting Optics for Use With Photovoltaic Cells 1299
A.K. Converse

Standardization of Data Sheet and Nameplate Specifications of Photovoltaic Modules 1303
W. Knaupp

Photovoltaic Lighting System Performance 1307
S.R. Harrington and T.D. Hund

Photovoltaic Module Energy Rating Methodology Development 1311
B. Kroposki, D. Myers, K. Emery, L. Mrig, C. Whitaker and J. Newmiller

A Development of Effective Test Method on Storage Batteries for PV Application 1315
K. Takigawa and H. Kobayashi

Photovoltaic Modules of "KVANT" With Improved Optical and Electrical Characteristics 1319
M. Kagan, V. Nadorov, V. Rjevsky and V. Unishkov

New Optical and Thermal Enhanced PV-Modules Performing 12% Better Under True Module Rating Conditions 1323
S. Krauter, R. Hanitsch and L. Moreira

Production Start-Up of 2 MW a-Si PV Manufacturing Line at Sovlux Plant 1327
M. Izu, X. Deng, H.C. Ovshinsky, R. Crucet, S.R. Ovshinsky and A. Polisan

Processing Evaluations of an Automated High-Throughput System for Interconnecting Crystalline Silicon Solar Cells 1331
M.J. Nowlan, S.J. Hogan, J.S. Patterson, S.F. Sutherland, J.M. Murach, W.F. Breen and G. Darkazalli

Reflectance-Reducing Covers for Solar Cells 1335
G.A. Landis

Reliability and Accelerated Life Tests of the AC Module Mounted OKE4 Inverter 1339
H. Oldenkamp, I.J. de Jong, C.W.A. Baltus, S.A.M. Verhoeven and S. Elstgeest

EMC of PV-Plants with Line-Commutated Inverters 1343
A. Kempe and U. Schönwandt

8. TERRESTRIAL SYSTEMS

The U.S. Utility Industry's Team-Up Commercialization Initiative: Program Implementation 1347
J. Bigger, K. Durand, S. Hester and J. Serfass

Photovoltaic Hybrid System Performance Comparisons: Prediction Versus Field Results 1353
S. Durand, A. Rosenthal and M. Thomas

Best Practices for Photovoltaic Household Electrification Programs 1357
A. Cabraal, M. Cosgrove-Davies and L. Schaeffer

A Bifunctional Utility Connected Photovoltaic System with Power Factor Correction and U.P.S. Facility 1363
S. Kim, G. Yoo and J. Song

Development of a Low Cost Integrated 15 KW A.C. Solar Tracking Sub-Array for Grid Connected PV Power System Applications 1369
M.J. Stern and R.T. West

An Evaluation of Integrated High-Concentration Photovoltaics for Large-Scale Grid Connected Applications 1373
V. Garboushian, D. Roubideaux, S. Yoon and J.A. Gunn

Test Results on DC Injection Phenomenon of Grid Connected PV System at Rokko Test Center 1377
A. Kitamura, F. Yamamoto, H. Matsuda, K. Akhmad and Y. Hamakawa

A Competition of Tracking Photovoltaic Systems in a Southwestern Electric Utility Transmission & Distribution Application 1381
T. Hickman, P. Eckert and T. Lepley

Characterizing (Rating) the Performance of Large Photovoltaic Arrays for all Operating Conditions 1385
D.L. King and P.E. Eckert

Direct Funding of Grid-Connected Photovoltaic Applications in Germany—An Overview 1389
K. Heidler

SINO/American Cooperation for PV Development in the People's Republic of China 1393
W.L. Wallace and Y.S. Tsuo

Photovoltaic R & D and Applications in Ghana Current Status and Prospects 1397
J. Essandoh-Yeddu

Niche Markets for Grid-Connected Photovoltaics 1401
H. Wenger, C. Herig, R. Taylor, P. Eiffert and R. Perez

The New German Electric Safety Standard for Residential PV Systems 1405
H. Laukamp

Codes, Standards and PV Power Systems A 1996 Status Report 1409
J. Wiles and W. Bower

Development of a 500 Watt Portable Thermophotovoltaic Power Generator 1413
F.E. Becker, E.F. Doyle, R. Mastronardi, K. Shukla, E.B. Linder and L.M. Garverick

Environmental Issues Related to Commercialization of $CuInSe_2$-Based Photovoltaics 1417
C. Eberspacher, V.M. Fthenakis and P.D. Moskowitz

Operation and Component Testing of a Solar Thermophotovoltaic Power System 1421
K.W. Stone, N.S. Fatemi and L.M. Garverick

Two-Loop Modular Solar Photothermal Plants 1425
VI. Kabakov

Maximum Power Point Tracking with Temperature Compensation of Photovoltaic for Air Conditioning System with Fuzzy Controller 1429
G.-J. Yu, M.-W. Jung, J. Song, I.-S. Cha and I.-H. Hwang

Roofing Material Integrated Flexible a-Si PV Modules 1433
T. Yoshida, M. Tanda, S. Kato, M. Horiguchi, Y. Watanuki, T. Hama, Y. Ichikawa, H. Sakai, N. Sakai, J. Kurihara and O. Ishikawa

PV Metal Roofing Module 1437
T. Ellison, L. Fatalski, R. Kopf, H. Ovshinsky, M. Izu, R. Souleyrette, K. Whelan, S.R. Ovshinsky, J. Wiehagen and L. Zarker

Energy Analysis of PV Cladding Systems 1441
K.M. Hynes, N.M. Pearsall, M. Shaw and F.J. Crick

Operation Behaviour of Roof Installed Photovoltaic Modules 1445
W. Knaupp

A New Method and System for the Simulation of Modular Inverters in Solar Façades 1449
G. Ebest, W. Hiller and U. Knorr

Validated Simulation for Thermal Regulation of Photovoltaic Wall Structures 1453
H.X. Yang, R.H. Marshall and B.J. Brinkworth

Experience with Building Integration of a Photovoltaic Facade 1457
H. Ossenbrink and C. Helmke

The Team-Up Commercialization Initiative: Progress of the Grid-Independent Program 1461
K. Durand, J. Bigger, S. Hester and J. Serfass

Opportunities and Issues in International Photovoltaic Market Development 1465
R. Taylor, D. Arent, S. Baldwin, R. McConnell, J. Stone, H. Ullal, C. Warner, W. Wallace, P. Klimas, E. Richards, C. Hanley and J. Strachan

PV-Hybrid Village Power Systems in Amazonia 1469
C.L. Warner, R.W. Taylor, C.M. Ribeiro, M. Moszkowicz and A.J.V. Borba

A Combined Technique for Elimination Of Islanding Phenomenon 1473
F.M.A. Ghali

Grid Connected Photovoltaic Supply Units for Railway Applications 1477
L. Lori, P. Redi and M. Ruzinsky

Techno-Economic Comparison of PV and Diesel Systems for Telecommunications and Aviation Navigational Aids 1481
U. Able-Thomas and R. Hill

A Study of Lead-Acid Battery Efficiency Near Top-of-Charge and the Impact on PV System Design 1485
J.W. Stevens and G.P. Corey

Evaluation of Solar Radiation Energy as a First-Hand Option in the Preliminary Evaluation of PV Pumping Systems 1489
N. Argaw

Photovoltaics in Poland 1493
S.M. Pietruszko and G. Wisniewski

Status and Interim Results From the Team-Up Grid-Connected Applications Program 1497
S. Hester, J. Bigger, K. Durand and J. Serfass

PG&E Experience with a 10-kW Commercial Rooftop PV System 1501
C. Jennings, J. Berdner, H. Wenger and C. Whitaker

Direct DC-DC Electric Vehicle Charging with a Grid Connected Photovoltaic System 1505
M. Vaidya, E.K. Stefanakos, B. Krakow, H.C. Lamb, T. Arbogast and T. Smith

The 2.1 kW Photovoltaic Electric Vehicle Charging Station in the City of Santa Monica, California 1509
J.G. Ingersoll and C.A. Perkins

PVUSA —The First Decade of Experience 1513
C. Jennings, B. Farmer, T. Townsend, P. Hutchinson, T. Reyes, C. Whitaker, J. Gough, D. Shipman, W. Stolte, H. Wenger and T. Hoff

The Value of Customer Preference 1517
C. Herig and A. Houston

A Learning Curve Approach to Projecting Cost and Performance in Thin Film Photovoltaics 1521
G. Cody and T. Tiedje

A Control System for Improved Battery Utilization in a PV-Powered Peak-Shaving System 1525
E. Palomino, J. Stevens and J. Wiles

The 25 Kilowatt SolarRow: A Building Block for Utility-Scale Concentrator Systems 1529
M.J. O'Neill and A.J. McDanal

Technical Evaluation of Two 6-kW Mono-Si Photovoltaic Systems at the National Renewable Energy Laboratory 1533
E. Ernest van Dyk, T. Strand and R. Hansen

Commercialization of a Value-Engineered Photovoltaic Tracking System 1537
D.S. Shugar, T. Hickman, P. Eckert and T. Lepley

PV-Friendly Pricing: The Commercialization of Grid-Tied PV Systems by Electric Utilities 1541
M.C. Russell and J. Hoffner

RAPID THERMAL PROCESSING OF CONVENTIONALLY AND ELECTROMAGNETICALLY CAST 100 cm^2 MULTICRYSTALLINE SILICON

S. Sivoththaman, W. Laureys, P. De Schepper, J. Nijs, R. Mertens
Inter-university Micro Electronics Center (IMEC), Kapeldreef-75, Leuven 3001, Belgium

ABSTRACT

100 cm^2 n^+pp^+ solar cells have been fabricated by rapid thermal processing (RTP) on conventionally cast (CC) and electromagnetically cast (EMC) multicrystalline silicon (mc-Si). All thermal steps were carried out by fast-ramp (>30°C/s) RTP using tungsten-halogen lamps. Emitter and BSF were simultaneously formed by RTP co-diffusion of phosphorous and boron / or aluminum (50 - 60 seconds) and surface passivation by rapid thermal oxidation, RTO (40 - 50 seconds). The all-RTP process resulted in 14.1% and 13.3% efficient cells on CC and EMC mc-Si respectively. The EMC cells, when subjected to an additional plasma hydrogen treatment, improved to give the same efficiency as the CC mc-Si cells. Systematic lifetime measurements performed on these materials show that the degradation in the EMC mc-Si is mainly due to the activated crystallographic defects, responding favourably to hydrogenation treatments but poorly to RT-gettering treatments. On the other hand, significant gettering effects are observed in CC mc-Si.

INTRODUCTION

Rapid thermal processing (RTP) is used in various stages of integrated circuit processing such as implantation damage anneal, silicidation, sintering, oxide anneals etc., where a low thermal budget is essential to have strict control on junction profiles and to avoid lateral dopant diffusions etc.. A more recent application of RTP is the development of silicon solar cells [1-5]. Recently we reported realisation of 15.4% efficient solar cells made entirely by RTP on 100 cm^2 industrial Cz-Si wafers [6]. The degradation in the bulk Si by the activation of crystallographic defects and residual impurities due to very fast temperature ramps is an issue of concern. These effects are expected to be minimal in single crystal Si. However, the case of mc-Si, which contains variety of inter-grain and intra-grain crystallographic defects and residual impurities is more complicated. Further, the grain structure and residual impurities (metals, O, C) depend also on the casting method used. In the present paper, we report on the response of differently cast mc-Si materials to fast-ramp RT-anneals, and on the presence of gettering effects during RT-dopant diffusion. Also reported is the performance of 100 cm^2 mc-Si cells fabricated by RTP without involving any conventional furnace processes.

EXPERIMENTAL

Investigation on minority carrier lifetime

To study the influence of RTP on the minority carrier lifetime of mc-Si wafers we chose two different kinds of materials from different manufacturers. One is conventionally cast (CC mc-Si) with larger grains (1.5 - 2 cm^2), while the other electromagnetically cast (EMC mc-Si) with very small (0.25 cm^2) grains. To take into account the lateral non-uniformities in the properties and to have a statistical approach, 100 cm^2 wafers were used.

Sample preparation

The surface damage of the as-cut wafers was first removed by removing 10-15 μm of Si from each side in a solution containing HNO_3:HF:CH_3COOH. The resulting surface was mirror-like. All the wafers were then subjected to a cleaning sequence, (i) $4H_2SO_4$:H_2O_2, (ii) $5H_2O$:NH_4OH:H_2O_2, (iii) $5H_2O$:HCl:H_2O_2 with 1% HF dips in between. Initial lifetime measurements were performed on all wafers (see section below). Following the lifetime measurements, another 1 -2 μm of Si was etched away from both surfaces of the wafers in a weak HF:HNO_3 solution, and the same cleaning sequence was performed again. The wafers were then divided into two groups: The first group of wafers underwent an RT-annealing (RTA) treatment in pure N_2 ambient. A commercial RTP furnace was used. All the quartzware was carefully etch-cleaned prior to the experiments to avoid any external contaminations. RT-anneals were performed in the temperature range 875-950°C for various samples. The temperature ramps were typically 50°C/s up and 30°C/s down. After the RTA treatments, the samples were cleaned again and lifetime measurements performed. For the second group of wafers, approximately 5000Å of phosphosilicate glass PSG (P_2O_5:SiO_2) was deposited on one side in an APCVD reactor at 400°C with SiH_4, PH_3, and O_2 as process gases. 1 μm of pure aluminum was then evaporated at 10^{-6} Torr on the other side of the wafers in an e-beam chamber. Rapid thermal diffusion (RTD) was then carried out using the same thermal cycles as before, simultaneously diffusing P and Al into the two sides of the wafers. Excess PSG and Al-Si alloy were stripped away in HF and HCl solutions respectively. At least 10 μm of Si was then removed from each side of the RT-diffused

0-7803-3166-4/96/$5.00 © 1996 IEEE

REC Exhibit 1013, Page 16 of 19

wafers in a polishing HNO_3:HF:CH_3COOH solution. All the wafers underwent the cleaning sequence once again and the lifetime measurements were performed on all group II wafers.

Carrier lifetime measurements

Time-resolved microwave photoconductivity (TRMC) measurements were used to evaluate the effective minority carrier lifetime (τ_{eff}) distributions. A μ-wave PCD measurement system with a laser beam of 1057 nm wavelength was used. The τ_{eff} that includes both the surface and bulk recombinations ($1/\tau_{eff} = 1/\tau_b + 1/\tau_s$) can be extracted from the decay of the μ-wave photoconductivity. In our case, the surfaces were passivated by 20 vol% HF. Measurements were performed on a large number of points in each wafer covering the whole 100cm^2 area. The diameter of the laser-illuminated area was approximately 2mm. For all wafers, τ_{eff} measurements were carried out before and after the RTP treatments with the surface preparations as described above.

Solar cell fabrication

Both conventionally cast (0.75, 0.9 and 2.8 Ω-cm), and electromagnetically cast (1 Ω-cm) mc-Si materials from different manufacturers were used to fabricate 100 cm^2 all-RTP cells. The wafers were saw-damage etched and cleaned as described above. For the emitter formation by RTD, APCVD deposited PSG was used as diffusion source. For the BSF, either APCVD borosilicate glass (BSG), or evaporated aluminum was used as RT-diffusion sources. The emitter and BSF were formed in a single RTD step in N_2 ambient. After removing the remains of the diffusion sources in appropriate chemical solutions, the samples were HF-dipped and rapid thermal oxidation (RTO) was carried out in an O_2 ambient for emitter surface passivation. During the RTO, 10 seconds before the end of the high temperature plateau, the ambient was switched back to N_2. Most of the RT-diffusions were carried out in the temperature range 900 - 925°C, for durations upto 60 seconds and the RT-oxidations at 900°C for upto 50 seconds. Some of the EMC wafers underwent a plasma hydrogenation treatment after the RTO. Direct hydrogenation was carried out from the rear side of the wafers in an rf (13.56 MHz) plasma system at 350°C. This treatment was limited only to the EMC wafers to see the effect of hydrogenation after the RTP treatments. The frontside contacts were formed by photolithography/lift-off technique and the rear contact was evaporated aluminum. Finally, a double layer antireflection coating of ZnS/MgF_2 was evaporated onto the frontside of the wafers.

RESULTS AND DISCUSSION

τ_{eff} after RTA without involving dopant diffusion

Figure 1 shows an example for the distribution of τ_{eff} in 100 cm^2 CC mc-Si before and after an RTA treatment of 925°C, 60s, without involving any dopant diffusion. Considerable diversity in τ_{eff} is observed in 100 cm^2 virgin wafers even before the RTP treatment. Regions of high and very low lifetimes are due to the randomness of various crystallographic defects and recombination centers in cast mc-Si material.

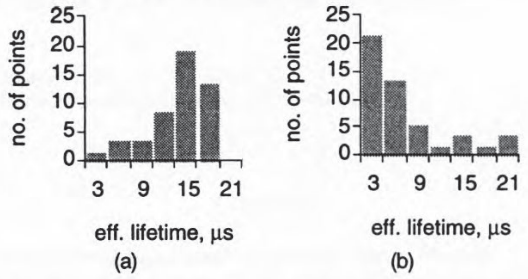


Figure 1. Distribution of τ_{eff} in CC mc-Si, (a) before, and (b) after an RTA treatment of 925°C, 60s, without involving any dopant diffusion

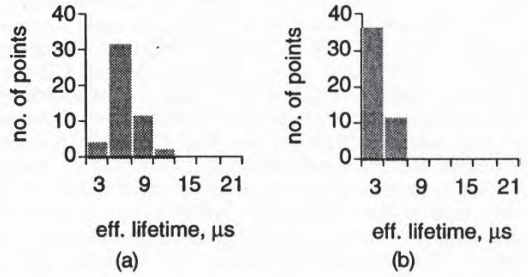


Figure 2. Distribution of τ_{eff} in EMC mc-Si, (a) before, and (b) after an RTA treatment of 925°C, 60s, without involving any dopant diffusion

From figure 1, it seems there occurred a severe lifetime degradation after the RTA treatment. More than half of the points measured showed τ_{eff} below 4 μs. Since external contamination in these experiments is highly unlikely, the main reason for the lifetime degradation should be the activation of crystallographic defects & metallic impurities as a result of quenching effect inflicted by the high cooling rates of >30°C/s. Similar degradations in τ_{eff} was also noted in the case of EMC mc-Si. Figure 2 shows the distribution bar-chart of τ_{eff} measured on EMC mc-Si before and after an RTA of 925°C, 60s. Due to the cold crucible casting method, it is generally beleived that the EMC mc-Si material contains much less amounts of oxygen and metallic impurities as compared to CC mc-Si material. However, the EMC mc-Si contains a very high density of grain- and sub grain-boundaries, whose activation due to the rapid thermal ramps might have contributed to the lifetime degradation after the RTA. Similar tendencies were observed in other temperatures as well. The above results indicate that RTA of mc-Si wafers without involving any dopant diffusion can result in strong degradations in minority carrier lifetime.

REC Exhibit 1013, Page 17 of 19

τ_{eff} after RT anneals involving dopant diffusion

Figure 3 shows the lifetime distribution of a CC mc-Si wafer before and after RT co-diffusion of phosphorous and aluminum (900°C, 50s.). Unlike the cases described above, when the RT annealing involved RT-diffusion of dopants such as P and Al, an improvement in τ_{eff} is noted. This evidences the presence of an RT-gettering effect after co-diffusion of P and Al. The resulting distribution chart after RTD shows a much wider spread in τ_{eff} as compared to the virgin wafers. Unlike what was reported for single crystal Si [7], some points still showed a degradation after the RTD treatment of CC mc-Si. This tendency was observed in all the CC mc-Si wafers that were subjected to RTD above 875°C.

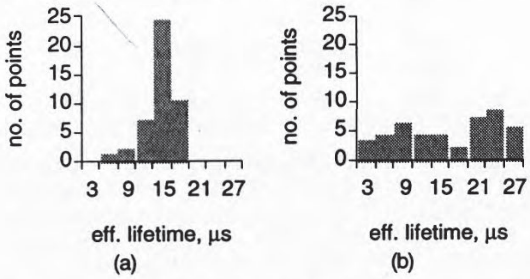


Figure 3. Distribution of τ_{eff} in CC mc-Si, (a) before, and (b) after an RT co-diffusion of P/Al at 925°C, 60s. (junctions were removed after RTD).

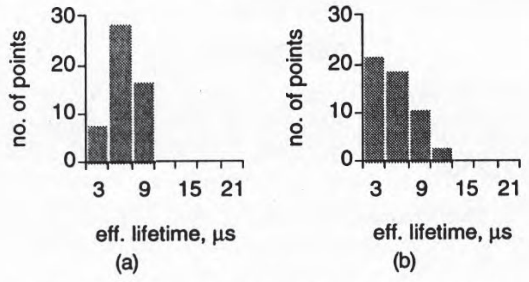


Figure 4. Distribution of τ_{eff} in EMC mc-Si, (a) before, and (b) after an RT co-diffusion of P/Al at 925°C, 60s. (junctions were removed after RTD).

Figure 4 shows a typical example of RTD gettering treatment on an EMC mc-Si wafer (900°C, 50s). In the case of EMC mc-Si, however, the improvement in τ_{eff} is not as pronounced as in the case of CC mc-Si. These results suggest that, (i) a strong gettering effect exists in the case of CC mc-Si after RT co-diffusion of P and Al, whereas this effect is very marginal in the case of EMC mc-Si, and (ii) the RT-induced degradations can be attributed to activation of residual impurities and/or crystallographic defects, the latter being more dominant in the case of EMC mc-Si, which might require treatments like hydrogenation for further improvement.

Performance of 100cm^2 RTP mc-Si cells

Table 1 shows the performance of the CC mc-Si cells fabricated by RTP. In the case of P and Al co-diffused samples, the RTO treatment increases the V_{oc} by more than 13 mV. The 40s RTO followed by 10s N_2 anneal results in good quality oxides. Ramping down in O_2 results in less good interface quality. Figure 5 compares the internal quantum efficiency (IQE) of two RTP CC mc-Si cells with and without RTO surface passivation. The blue response is further increased by the RT-oxidation of the shallow emitter surface. RTO treatment was found to be beneficial for p-type (boron) emitters as well [8].

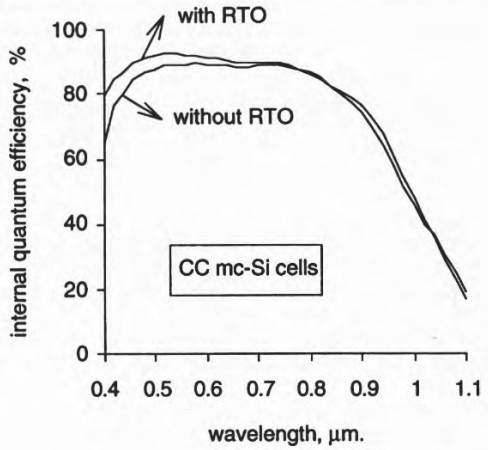


Figure 5. Internal quantum efficiency (IQE) of two RTP CC mc-Si cells showing the effect of RTO surface passivation

In Table 1, the comparison between the n^+pp^+ (P/Al) and n^+p cells show also the beneficial effects of aluminum. However, the 2.8 ohm-cm mc-Si material did not give a high enough V_{oc} with an oxide passivated n^+pp^+ strucrute, even though it gave the highest J_{sc}. One of the reasons for the low V_{oc} may be higher base saturation currents due to low substrate doping level. The main results of the EMC mc-Si cells are given in Table 2. The improvement brought about by the hydrogen plasma treatment is quite large. Figure 6 compares the IQE of two RTP EMC mc-Si cells with and without hydrogen passivation. From Table 2, it seems that the incorporation of aluminum BSF does not help much in the EMC cell performance. Comparing these results with the lifetime measurements mentioned above, it seems that RT-induced degradation can be conveniently minimized to acceptable levels by RT-gettering of metallic impurities in the case of large grain CC mc-Si materials. For EMC mc-Si, however, treatments like hydrogenation might be necessary to recover the degradations in materials like EMC mc-Si which contains a large density of grain boundaries and crystallographic defects, whose activation can be the main mechanism for the τ_{eff} degradation.

REC Exhibit 1013, Page 18 of 19

Table 1. Performance of 100 cm^2 RTP CC mc-Si cells

Resistivity (Ω-cm)	structure	dopant(s)	RTD T(°C) / t(s)	RTO T(°C) / t(s)	J_{sc} (mA/cm^2)	V_{oc} (mV)	FF (%)	η (%)
0.75	n^+pp^+	P/B	925/60	900/50	31.4	595	75.1	14.0
0.90	n^+pp^+	P/Al	925/50	925/50	30.8	592	77.3	14.1
0.90	n^+pp^+	P/Al	925/50	925/50	30.5	592	77.3	13.9
0.90	n^+p	P	925/50	925/50	29.7	587	77.1	13.4
0.90	n^+pp^+	P/Al	925/50	-	30.2	579	76.1	13.3
2.8	n^+pp^+	P/Al	900/50	900/50	32.2	581	75.2	14.1

Table 2. Performance of 100 cm^2 RTP EMC mc-Si cells

structure	dopant(s)	plasma hydrogen	RTD T(°C) / t(s)	RTO T(°C) / t(s)	J_{sc} (mA/cm^2)	V_{oc} (mV)	FF (%)	η (%)
n^+pp^+	P/Al	no	925/50	900/50	29.6	583	76.9	13.3
n^+p	P	yes	925/50	900/50	30.8	595	76.6	14.0
n^+pp^+	P/Al	yes	925/50	900/50	30.9	593	77.1	14.1

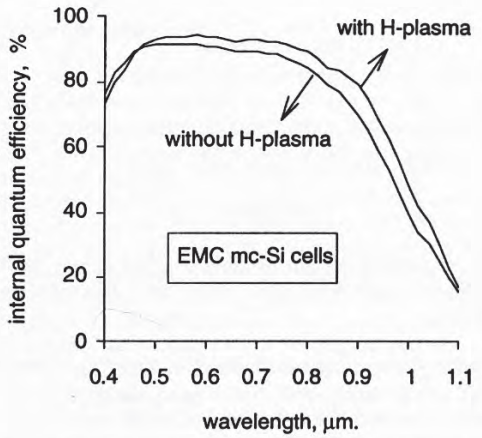


Figure 6. Internal quantum efficiency (IQE) of two RTP EMC mc-Si cells showing the effect of hydrogen plasma passivation

In general, the J_{sc} values obtained in all our mc-Si cells seem quite moderate. Better surface texturing and/or optical confinement techniques can further improve J_{sc}.

CONCLUSIONS

The influence of RTP treatments on minority carrier lifetime of mc-Si materials has been studied. RT anneals, when not accompanied by diffusion of dopants such as P and/or Al, cause serious degradation in minority carrier lifetime by RT-induced activation of impurities, grain boundaries, and other crystal defects. Significant impurity gettering effects have been observed in large grain mc-Si material, whereas small grain EMC material was not very sensitive to gettering treatments. On the other hand, grain boundary passivation by hydrogenation treatment is very efficient in the case of EMC material. 100 cm^2 mc-Si cells have been fabricated using only rapid thermal processes. n^+pp^+ cells with RTO surface passivation demonstrated >14% conversion efficiencies, using CC mc-Si wafers. Comparable efficiencies have been obtained with all-RTP EMC mc-Si cells after a plasma hydrogenation treatment.

Acknowledgement: Work supported by EC Contracts JOU2-CT92-0179 MultiCHESS and JOR3-CT95-0069 LowThermCells. K. Said is thanked for help in the spectral response measurements.

REFERENCES

[1] R. Schindler, I. Reis, B. Wagner, A. Eyer, H. Lautenschlager, C. Schetter, W. Warta, B. Hartiti, A. Slaoui, J. C. Muller, P. Siffert, *23rd IEEE PVSC*, 1993, pp. 162-166.

[2] S. Sivoththaman, B. Hartiti, J. Nijs, A. Barhdadi, M. Rodot, J. Muller, W. Laureys, D. Sarti, *12th EC PVSEC*, 1994, pp. 47-51.

[3] A. Rohatgi, Z. Chen, P. Doshi, T. Pham, D. Ruby, *Appl. Phys. Lett.* **65**, 1994, pp. 2087-2089

[4] S. Sivoththaman, W. Laureys, J. Nijs, R. Mertens, *Appl. Phys. Lett.* **67**, 1995, pp.2335-2337.

[5] A. Beyer, G. Ebest, R. Reich, *Appl. Phys. Lett.* **68**, 1996, pp.508-510

[6] S. Sivoththaman, W. Laureys, P. De Schepper, J. Nijs, R. Mertens, *13th EC PVSEC*, 1995, pp. 1574-1577.

[7] B. Hartiti, A. Slaoui, J.C. Muller, P. Siffert, *Appl. Phys. Lett.* **63**, 1993, pp. 1249-1251.

[8] S. Sivoththaman, W. Laureys, J. Nijs, R. Mertens, *MRS Proceedings*, **387**, 1995, pp.259-264

REC Exhibit 1013, Page 19 of 19